BUTTERWORTH HEINEMANN

Polymer Vol. 36 No. 24, pp. 4579–4585, 1995

0032-3861/95/$10.00+0.00

Thermal, mechanical and dielectric studies of a metallomesogenic polyester

J. A. Puértolas*
Dpto Ciencia de Materiales, Centro Politécnico Superior, Instituto de Ciencias de Materials de Aragón, Universidad de Zaragoza, CSIC, 50015 Zaragoza, Spain

and R. Díaz Calleja
Dpto Termodinámica Aplicada, Escuela Superior de Ingenieros Industriales, Universidad Politécnica de Valencia, Spain

and L. Oriol
Dpto Química Orgánica, Escuela Universitaria Politécnica de Huesca, Instituto de Ciencias de Materiales de Aragón, Universidad de Zaragoza, CSIC, 22071 Huesca, Spain
(Received 11 April 1994; revised 9 March 1995)

The characterization of a main-chain metallomesogenic polyester has been carried out by differential scanning calorimetry, dielectric relaxation spectroscopy and dynamic mechanical analysis. The mesogenic repeat unit of the polyester derived from a salicylaldimine copper(II) complex shows a nematic phase like conventional organic liquid-crystal polymers. This semicrystalline polymer displays a set of different relaxation processes, such as β relaxation, α relaxation, melting process, cold crystallization effects and conductivity contributions, which have been carefully studied.

(Keywords: metallomesogenic polyester; dielectric relaxation; dynamic mechanical analysis)

INTRODUCTION

The high level of interest in liquid-crystal polymers (LCP) lies in their properties, which mostly derive from the molecular orientation in the liquid-crystalline state. The molecular structures of LCP have usually been based on fully organic mesogenic molecules.

During the last few years there has been increasing interest in metal-containing liquid crystals, which are known as metallomesogens[1,2]. These new materials open new structural possibilities derived from the coordination chemistry. A large number of new mesogenic molecules can be developed by using adequate ligands and metal ions. Furthermore, the metal atom is characterized by a large and polarizable electron density, which will have profound effects on the physical properties of the liquid crystal. Unlike the high number of low-molecular-weight metallomesogens described so far, little is known about metal-containing LCP or metallomesogenic polymers. Metal-containing polymers are interesting materials owing to their applications, e.g. molecular electronics[3], catalysis[4], non-linear optics[5] or organic-based magnets[6].

The incorporation of metal ions into polymeric chains to obtain metallomesogenic polymers gives rise to different and attractive expectations apart from their academic interest. Thus, new physical properties and potential applications can derive from the presence of metals in ordered fluid phases. These properties can be combined with the processing of polymers (e.g. oriented films or fibres). Coloured polymers, materials with long-range magnetic order[7], supramolecular and organized structures for optoelectronic applications[8], third-order non-linear optical materials[9] or even the improvement of the processability of high-performance aramids by organometallic modifications[10] are some reported examples of the above-mentioned possibilities.

The few reported examples of metal-containing LCP include lyotropic[11] and thermotropic[12] polymers, as well as elastomers[13] and ionomers[14]. This paper deals with a metallomesogenic polyester derived from a Schiff-base copper(II) complex shown in *Figure 1*.

In previous papers[15,16] we described the synthesis and mesogenic behaviour of a series of this kind of homopolymer. The polyester was obtained by interfacial polycondensation of a functionalized copper(II) complex and an acid dichloride. Depending on the N-substituent of the copper(II) salicylaldiminate monomers and the acid dichlorides (aliphatic or aromatic with different flexible spacers) used in the polymerization, different series of metallomesogenic polymers can be obtained. Because of the square-planar coordination of the copper(II) complex, these polymers exhibit mesogenic properties (nematic phase). The thermal stability of the mesophase depends on the rigidity of the polymeric chain. In a recent paper[17] we have described the magnetic properties of these polymers and also the characterization of fibres drawn from the nematic melt.

This work is mainly focused on the dielectric and

* To whom correspondence should be addressed

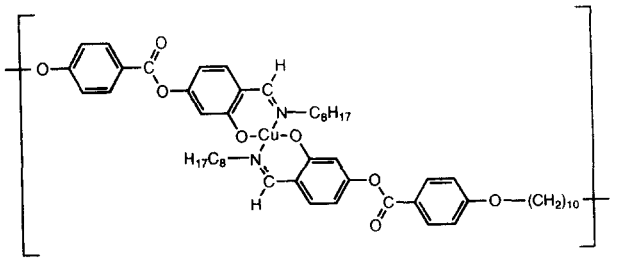

Figure 1 Repeat unit of the metallomesogenic polyester

mechanical behaviour of this metallomesogenic polymer. Most of the studies of correlations between relaxation processes and motion of dipolar groups are concerned with side-chain and combined side-group main-chain LCP[18], and only a few examples of main-chain LCP have been reported[19]. A more complex thermal behaviour, associated in part with the tendency to crystallize and also with the high mesophase temperatures, introduces some difficulties in the characterization of the relaxations. Therefore, a detailed thermal analysis is necessary before performing the dielectric measurements. In addition, the presence of Cu(II) moieties at high temperatures causes poor stability under an electric field[15], which hinders the dielectric relaxations present in this polymer. In our case, dynamic mechanical analysis (d.m.a.) proves to be a useful complementary technique to study the molecular dynamics.

EXPERIMENTAL

The synthesis and characterization data of the polymer were previously reported[16]. An inherent viscosity $\eta_{inh} = 0.15$ was determined with a Cannon-Fenske viscosimeter at a concentration of 0.5 g dl^{-1} in 1,2,2,2-tetrachloroethane at 50°C.

Thermogravimetric analysis (t.g.a.) was carried out with a Perkin-Elmer TGS-2 equipped with a System 4 microprocessor controller at 10°C min^{-1} in nitrogen atmosphere from 40 to 600°C. The atmosphere was changed at 600°C (inert to oxidation) and a strong decomposition took place. The inorganic residue at 750°C, CuO, allowed us to determine a copper content of 6.77% according to the calculated value.

D.s.c. measurements were performed with a Perkin-Elmer DSC-2 or DSC-7 calibrated with indium and tin. Transition temperatures were read at the maximum of the transition peaks. Glass transitions were measured at the midpoint of the heat-capacity increase. Mesogenic behaviour was studied with a Nikon polarizing microscope fitted with a Mettler FP-82 heating stage and an FP-80 control unit.

Dielectric measurements have been performed using a TA Instruments DEA 2970 over 1 mm thick and 20 mm diameter discs, sintered from powdered compound heated above its melting point and cooled down at a moderate rate. The measurements were made at a heating scan rate of 1°C min^{-1} from −130 to 180°C, sweeping the frequency in the range 0.1 Hz–30 kHz.

Dynamic mechanical measurements were carried out with a Rheometrics DMTA Mark II in bending on prismatic test specimens of area $1 \times 10\,mm^2$, sintered by the former method. The two heating runs were made at a rate of 1°C min^{-1} from −130 to 160°C. The frequencies used were 0.1, 0.3, 1, 3 and 10 Hz.

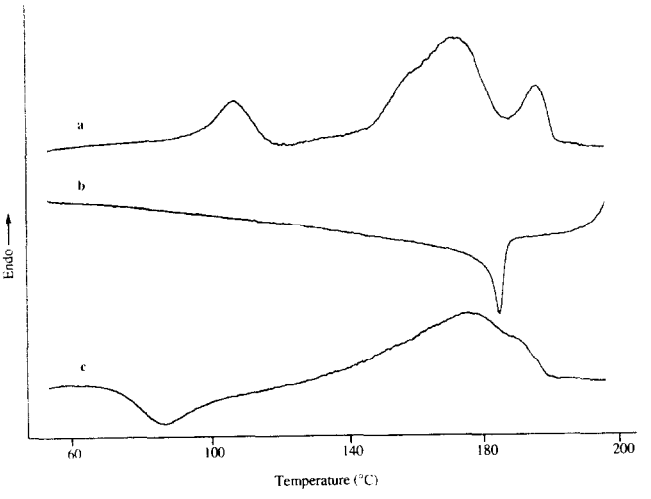

Figure 2 D.s.c. traces of the polymer: (a) first heating run; (b) first cooling run; (c) second heating run. Scan rate = 10°C min^{-1}

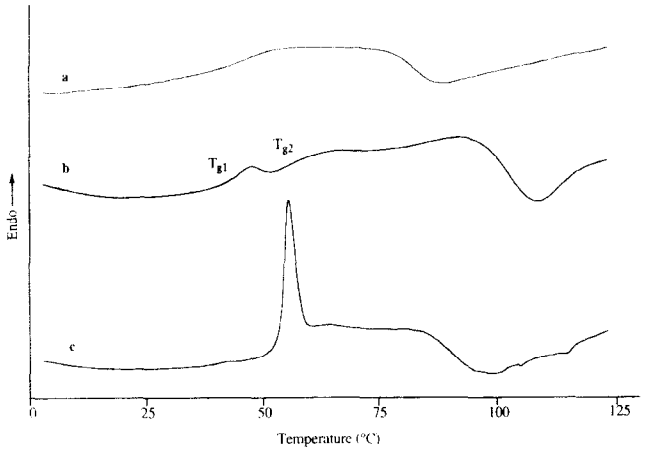

Figure 3 D.s.c. traces of the polymer in the glass transition region: (a) sample cooled at 10°C min^{-1} from the isotropic melt to −60°C; (b) sample quenched from isotropic melt into liquid nitrogen; (c) sample quenched from isotropic melt into liquid nitrogen and annealed at room temperature for a long time. Heating rate = 20°C min^{-1}

RESULTS AND DISCUSSION

D.s.c. and optical microscopy measurements

The polymer showed good thermal stability with the onsets of the decomposition curve at 297°C and 355°C. No weight loss was detected before decomposition.

Optical microscopy reveals an enantiotropic nematic mesophase by heating a sample of polymer as prepared. Threaded (closed loops) and marbled nematic textures were characterized. Furthermore, these nematic textures can be retained at room temperature by cooling the nematic melt.

D.s.c. measurements showed two broad peaks corresponding to melting and isotropization transitions at $T_m = 174$°C and $T_i = 197$°C, respectively, on the first heating. The thermodynamic data corresponding to the nematic–isotropic liquid transition (N–I) were: $\Delta H_{N-I} = 5.2\,kJ\,mru^{-1}$ and $\Delta S_{N-I} = 11.0\,J\,K^{-1}$ (mru = moles of repeat units). These values are very similar to the literature data for semiflexible organic nematic polymers with an even number of carbon atoms in the flexible spacer. On the cooling run an exothermic peak corresponding to an isotropic–nematic transition was

found at 185°C (hysteresis), but no crystallization was observed at lower temperatures. Consequently, on the subsequent heating run a cold crystallization was observed prior to a broad and complex peak that includes melting and isotropization transitions. The maximum of this peak at 177°C can be assigned to T_m. Nematic–isotropic liquid transition was detected as a shoulder at 191°C according to the optical microscopic observations. All these transitions are plotted in *Figure 2*. The broadness of the thermal transitions can be justified by the polydispersity of this unfractionated sample.

To characterize the glass transition and the above-mentioned cold crystallization of the amorphous regions, samples with different thermal histories have been studied. *Figure 3a* shows the d.s.c. trace of a sample cooled from the isotropic melt (220°C) to −60°C at 10°C min^{-1} and rerun (heating rate = 20°C min^{-1}). A glass transition at about 40°C and a cold crystallization at about 95°C can be observed. The same behaviour was shown by samples cooled at 20°C min^{-1} and even by samples quick cooled from the isotropic melt (this thermal treatment was made in the calorimeter). Besides, similar d.s.c. traces were obtained when the samples were cooled from the nematic melt at 185°C.

Samples quenched from the isotropic melt to liquid-nitrogen temperature and rerun showed a complex glass transition region followed by a cold crystallization. Two separate glass transitions can be observed at $T_{g1} = 41$°C and $T_{g2} = 57$°C, which may be attributed to two different amorphous regions corresponding to the liquid-crystalline state and the isotropic state[20] (*Figure 3b*). Contributions of different mobile structural moieties in each glass transition have been pointed out in a previous paper[16]. When the samples were annealed for a long time at a temperature (room temperature) lower than T_g, the d.s.c. trace displays a glass transition coupled with an endothermic peak. This behaviour has been defined as 'structure recovery' by Kovacs *et al.*[21] (*Figure 3c*).

In conclusion, the isotropic state can be frozen by quenching into liquid nitrogen, but, even in this case, it is not possible to avoid completely the isotropic–liquid crystal transition. In the rest of the samples, a nematic glass was obtained by cooling the isotropic melt, or nematic melt, at a moderate rate. Furthermore, the two glass transitions detected in the quenched sample are assigned as T_{g1}, corresponding to a nematic glass, and T_{g2}, corresponding to an isotropic glass.

Dielectric relaxation measurements

The dielectric study was carried out from the measurements of the complex dielectric constant, ϵ^*, as a function of temperature from −130 to 180°C and at various frequencies in the range 0.1 Hz–30 kHz. The results are separated to two temperature ranges that correspond to the presence of two different kinds of relaxation.

The examination of the thermal variation of $\epsilon'(T)$ and $\epsilon''(T)$ in *Figures 4a* and *4b* reveals a shallow relaxation that takes place over a temperature range from −130°C up to 20°C. It is reflected by means of a stepwise behaviour in $\epsilon'(T)$, with low values of the strength, according to the dipolar structure of the polymer. On the other hand, the dielectric loss curves suggest a single and

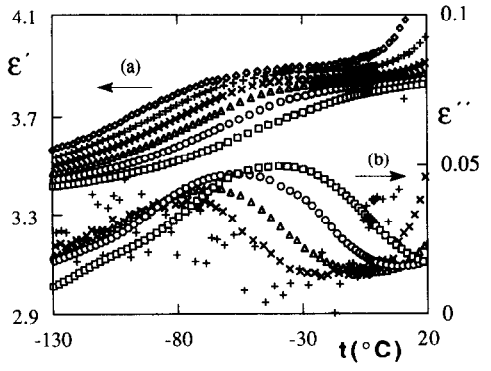

Figure 4 Temperature dependence of (a) real part of the complex dielectric function $\epsilon'(T)$ and (b) dielectric loss factor $\epsilon''(T)$ at different frequencies: 0.1 Hz (◇), 1 Hz (+), 10 Hz (×), 100 Hz (△), 1000 Hz (○), and 10 kHz (□)

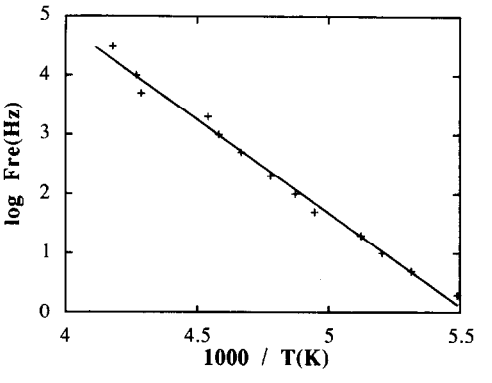

Figure 5 Arrhenius plot for isochronal temperature sweeps

distinct maximum for each frequency whose intensity decreases when the frequency decreases. An initial analysis of the character of this relaxation seems to show that it corresponds to a secondary relaxation since it appears at a temperature range below the glass transition. As a consequence of the method of preparation of the sample, this glass transition corresponds to T_{g1}, according to the d.s.c. measurements.

An Arrhenius representation (*Figure 5*) of the frequency *versus* temperature maximum (isochronal basis) provides a straight line, which confirmed that this transition may be associated with a β relaxation. The values of the molar activation energy $Q = 14.4$ kcal mol^{-1}, obtained by fitting the data in the range −100 to −40°C, also point out the same assignment of the relaxation.

In order to extend the characterization of this relaxation, we carried out a frequency analysis from the isothermal plots, $\epsilon'(\omega)$ and $\epsilon''(\omega)$, represented in *Figures 6* and *7*. The curves describe the presence of the relaxation, at high enough temperatures, although they show an increase at low frequencies that may be attributed to a conductivity contribution or to the following dipolar mechanism. This effect, although low, seems to be predominant at temperatures below −90°C. This behaviour, in particular $\epsilon'(\omega)$, does not allow us to use constant-temperature Argand plots (ϵ'' vs. ϵ') to obtain the relaxation parameters in a better way.

We discuss our data of $\epsilon''(\omega)$ in terms of the usual

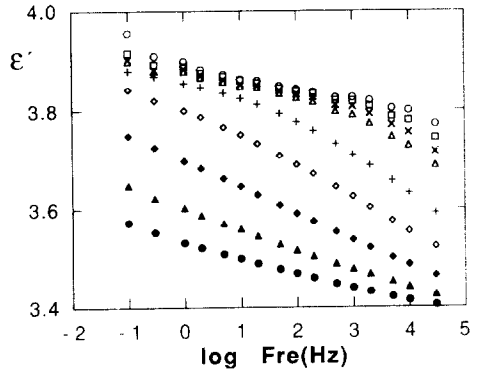

Figure 6 Frequency dependence of the real part of the dielectric constant, $\epsilon'(\omega)$, at different temperatures: 0°C (○), −10°C (□), −18°C (×), −25°C (△), −50°C (+), −70°C (◇), −90°C (◆), −110°C (▲), −130°C (●)

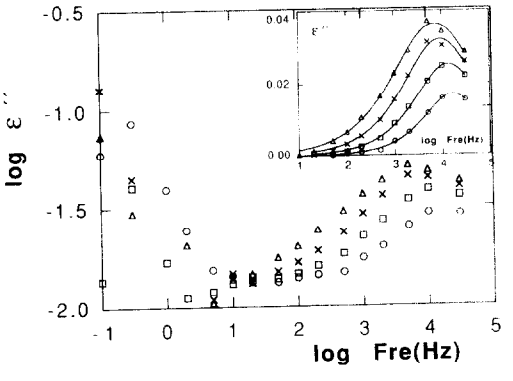

Figure 7 Dependence of ϵ'' as a function of frequency ω at different temperatures: 0°C (○), −10°C (□), −18°C (×), −25°C (△). Inset: ϵ'' after background is removed; the full curves are the Cole–Cole fit

expression that describes the frequency dependence of the dielectric loss constant in the vicinity of dipolar absorption for a secondary relaxation. Therefore, we used the Cole–Cole formula:

$$\epsilon'' = \mathrm{Im}\left(\epsilon_u + \frac{\epsilon_r - \epsilon_u}{1 + (i\omega\tau_0)^{1-\alpha}}\right) \qquad (1)$$

in which τ_0 is the relaxation time of the process, α is a dimensionless parameter related to the width of the relaxation-time distribution, and ϵ_u and ϵ_r are the unrelaxed and relaxed values of the dielectric constant, respectively. The fit of ϵ'', after correcting the background, is drawn in the inset of *Figure 7* by full curves. The results show a strong dependence on temperature for the broadening parameter α and values of the relaxation strength $\epsilon_r - \epsilon_u$ less than the approximately 0.3 deduced from $\epsilon'(T)$, which is due in part to the inaccuracy of the frequency of the maximum in $\epsilon''(\omega)$ used in the fit. Below −50°C, the increase of ϵ'' at low frequency masks the process and makes difficult an analysis of the relaxation times, which shift to high values when the temperature decreases.

Bearing in mind the structure of the polymeric chain, which has a rigid metallomesogenic core derived from a Schiff-base copper(II) complex, the former β relaxation could be assigned to motions involving the 4-alkoxybenzoate units in the case of end-groups. The latter behaviour could be due to the low degree of polymerization inferred from the low inherent viscosity value of this

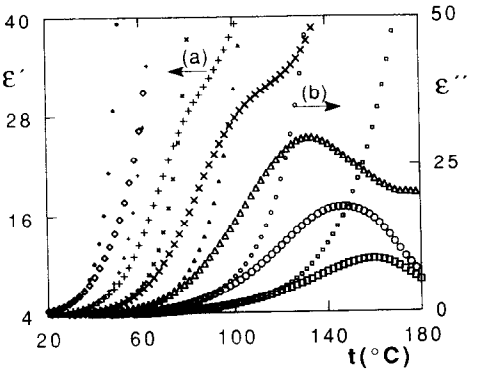

Figure 8 Thermal variation of (a) $\epsilon'(T)$ (large symbols) and (b) $\epsilon''(T)$ (small symbols) at different frequencies: 0.1 Hz (◇), 1 Hz (+), 10 Hz (×), 100 Hz (△), 1 kHz (○), 10 kHz (□)

oligomeric polymer. If one assumes that resonance stabilization at the carbonyl sites can prevent rotation about the carbonyl–aromatic carbon bonds[22], then motion of the permanent dipoles is only possible by rotation at the other oxygen–aromatic carbon or oxygen–aliphatic carbon.

On the other hand, the activation energy corresponding to this Arrhenius-type β relaxation is about 14 kcal mol^{-1}. This value is similar to the one found in 4-hydroxybenzoic acid homo- and copolymers reported by Kalika *et al.* [23,24], and corresponds to the dielectric rotational 4-hydroxybenzoate units, in other words, to the motions of the ester groups that occur in non-crystalline regions of the sample.

As far as the high-temperature dielectric behaviour is concerned, we should expect an α process in the temperature range around T_g. However, the dielectric features are more complex. Thus, when the sample is heated from low temperature and immediately goes over the β relaxation peak, the loss factor $\epsilon''(T)$ (see *Figure 8b*) increases monotonically and sharply without reaching any maximum. The range of temperature in which this rise occurs is approximately above 20°C. This behaviour is related to the initial change in the baseline of d.s.c. curves, corresponding to the glass transition, and therefore also related to the rise of free volume, which introduces more molecular mobility for the dipoles and ions. A further frequency analysis of $\epsilon''(\omega)$ clearly indicates that this increase corresponds to a conduction contribution overlapped with a dipolar relaxation.

The thermal variation of $\epsilon'(T)$ is plotted in *Figure 8a*. A similar type of rise as in $\epsilon''(T)$ appears in $\epsilon'(T)$, only at around 0.1 Hz. However, at higher frequencies some competitive processes can be considered. One of these processes is evidently the α relaxation that provides a stepwise behaviour when the conduction effects disappear, e.g. at high frequencies. However, another process has to contribute because $\epsilon_s(T)$ strongly reduces when the frequency increases. When both processes overlap, the existence of an unusual broad peak in $\epsilon'(T)$ is clearly in evidence.

It seems logical to think that, above the glass transition, the above-mentioned increase of mobility produces an increment in $\epsilon'(T)$. However, the subsequent decrease generating a peak is less common. A possible interpretation could be related to the presence of the exothermic peak around 100°C reflected in the d.s.c.

trace, which corresponds to a further cold crystallization of the sample after passing through the glass transition on heating. The loss in mobility associated with the reduction of the amorphous region in the semicrystalline polymer could decrease the value of the dielectric constant. On the other hand, the dynamics of the crystallization process is reflected in the variation shown by the strength and the temperature of the maximum as a function of the frequency.

The plot of log ϵ'' *versus* log ω, in the temperature range studied, shows, first of all, the existence of a constant d.c. conductivity, σ_{dc}. This contribution gives a dependence of ϵ'' proportional to $1/\omega$ and appears in this representation as a straight line with a slope of -1. At higher temperatures only this mechanism is present. However, when the temperature decreases there is a substantial deviation from this slope at high frequencies. This behaviour corresponds to another loss process, which shifts towards low frequencies. In order to analyse this mechanism we have to subtract the background contribution. If we draw the new values of ϵ'' in the same type of plots, the appearance of a new linear region would point out the presence of a hopping conductivity due to mobility of charge carriers in an amorphous disordered conductor[25]. This conductivity has the following frequency dependence, $\sigma = \sigma_\omega \omega^s$ with $0 < s < 1$, and contributes to the loss constant through the expression:

$$\epsilon'' = \sigma/(\epsilon_0 \omega) = \sigma_\omega \omega^{s-1}/\epsilon_0 \qquad (2)$$

When the level of this conductivity term is rather high, an alternative method of analysis consists of using the plot log σ vs. log ω. This graph provides a horizontal straight line for the frequencies in which the d.c. conductivity is predominant, and regions with slope s when the hopping conductivity effect is predominant. This effect shifts towards low frequencies when the temperature decreases. *Figure 9* shows clearly that only both behaviours are present at temperature above 80°C. In the same figure we also plot data fitted to the expression:

$$\sigma = \sigma_{dc} + \sigma_\omega \omega^s \qquad (3)$$

The values obtained for s are around 0.5–0.6 with a weak temperature dependence. Because these values are lower than those for other main-chain polymers[26], we

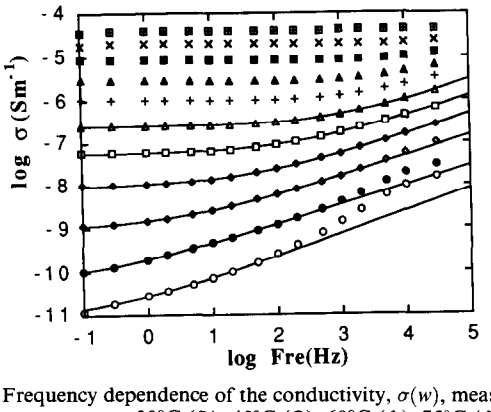

Figure 9 Frequency dependence of the conductivity, $\sigma(w)$, measured at different temperatures: 30°C (○), 45°C (●), 60°C (◇), 75°C (◆), 90°C (□), 105°C (△), 121°C (+), 134°C (▲), 150°C (■), 165°C (×), 179°C (⊞). The full curves are the fit to equation (3)

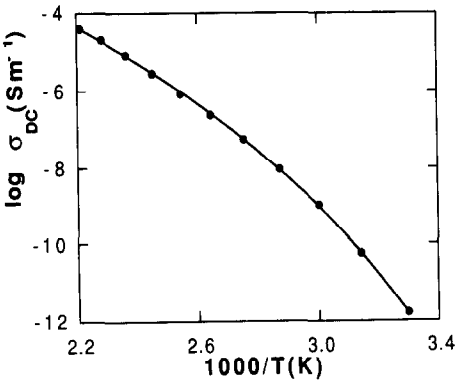

Figure 10 Arrhenius representation of σ_{dc} obtained by fitting our data of $\sigma(\omega)$ according to equation (3)

cannot reject the possibility of attributing this effect to interfacial polarization at partly blocking electrodes[27], rather than hopping processes. The fit gives amplitudes σ_ω with a strong temperature dependence like the σ_{dc} conductivity.

In order to study the temperature behaviour of the former contribution, σ_{dc}, the data have been drawn in an Arrhenius plot (*Figure 10*). However, the shape of the curve is most like that of a Williams–Landel–Ferry rather than an Arrhenius law. Fitting $\log \sigma_{dc}$ to the expression $C_1(T - T_0)/(C_2 + T - T_0)$, we obtained a value of $T_0 = 85$°C, a temperature higher than the glass transition observed in d.s.c. This behaviour, although it is not usual, appears in other materials such as alkali salt complexes, in which an increase in conductivity with the same temperature dependence is observed above the glass transition temperature of the polymeric matrix[28].

Another loss process appears below 80°C, since the curves present a strong variation of slope with frequency. In order to evaluate the contribution of this new process, the previous effects must be removed. We chose, *a priori*, a range of low frequencies in which we can suppose that this process has no contribution. This range always corresponds to low frequencies and it narrows when the temperature decreases. Using the same kind of fit as for high temperatures, we obtained the curves depicted by full curves in *Figure 9*. These curves show evidence of this process, which is associated with the α relaxation. The obtained values for α_{dc} are drawn in *Figure 10*. This figure clearly points out that some precautions have to be taken when extrapolation at low temperature of the Arrhenius law is carried out in order to evaluate d.c. conductivity in regions in which other contributions are present.

A way to confirm if the previous method is correct consists of evaluating the contribution of $\sigma_\omega \omega^s$ to the real part of the complex constant. For $\epsilon'' = \sigma_\omega \omega^{s-1}/\epsilon_0$ the corresponding real part using the Kramers–Kronig relations takes the form;

$$\epsilon' = \tan(s\pi/2)\sigma_\omega \omega^{s-1}/\epsilon_0 \qquad (4)$$

The fit of our data is represented in *Figure 11* and the values of s and σ_ω are in accordance with those obtained in the analysis of $\epsilon''(\omega)$ at the same temperatures. At higher temperatures the decrease of ϵ' related to the cold crystallization process did not allow the same comparison to be made.

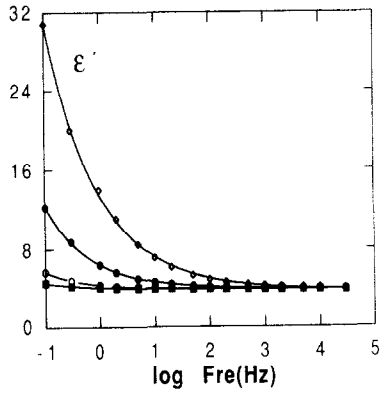

Figure 11 Dependence of ϵ' as a function of the frequency ω, at different temperatures: 20°C (■), 30°C (○), 45°C (●), 60°C (◇). The full curves are calculated from ϵ'' by equation (4) without adjustable parameters

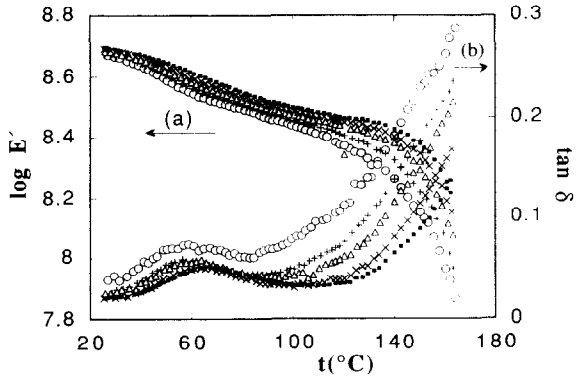

Figure 12 Thermal dependence of (a) and E' and (b) tan δ in the first heating run at different frequencies: 0.1 Hz (○), 0.3 Hz (+), 1 Hz (△), 3 Hz (×) and 10 Hz (■)

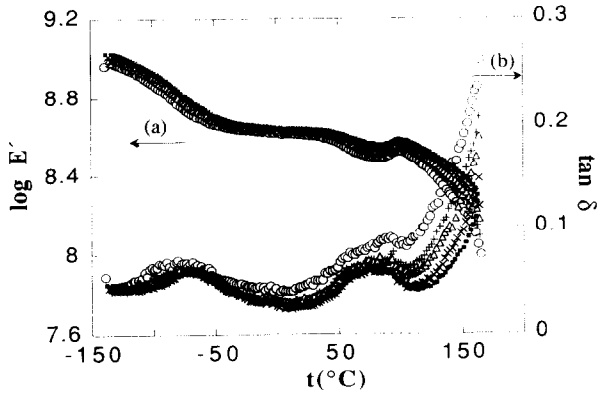

Figure 13 Thermal dependence of (a) log E' and (b) tan δ in the second heating run at different frequencies: 0.1 Hz (○), 0.3 Hz (+), 1 Hz (△), 3 Hz (×) and 10 Hz (■)

We have tried to fit the $\epsilon''(\omega)$ data after correcting the previous conductivity contributions. However, we cannot make any fit to an empirical equation, using either the modulus or impedance representations, owing to the presence of the cold crystallization effects. Some fits, by means of a Havriliak–Negami relation according to the character of this process, gave no acceptable results for the parameters of this relaxation. On the other hand, the frequency range in which that process emerges is limited. Furthermore, the values of conductivity above 70°C are so strong that no qualitative analysis is possible. For this reason, a dynamic mechanical analysis has been carried out to gain information on the dipolar relaxation processes without the presence of the conductivity.

Dynamical mechanical measurements

Two different temperature scans were made at five constant frequencies, from 0.1 to 10 Hz, over a wide range of temperature. The first heating run was carried out from room temperature to 180°C. The thermal variations of the elastic modulus, E', and the loss tangent, tan δ, are reflected in *Figures 12a* and *12b*. A smooth decrease of E' around 60°C and a peak of tan δ in the same region can be observed. This behaviour is associated with the α relaxation, which confirms the process found in dielectric measurements. However, this process is detected more easily by mechanical rather than dielectric measurements. The strong drop in log E' and the sharp rise in tan δ around 150°C correspond to the beginning of the transition to a nematic melt, in accordance with d.s.c. measurements.

The second heating scan was carried out from −150 to 160°C, after cooling the sample inside of the cell. The results, plotted in *Figures 13a* and *13b*, provide new arguments to correlate dielectric and mechanical measurements. Thus, in addition to the previously mentioned α relaxation and melting transition, two new processes appear. One of them is located below the glass transition above −90°C and the other one around 100°C.

The first one is detected by a strong decrease in log E' and a peak in δ, and can be attributed to the β relaxation according to the temperature region in which it appears. Furthermore, the values of the activation energy, 14–15 kcal mol^{-1}, obtained by Arrhenius plots from the maximum of the isothermal curves of E'' and tan δ at different frequencies, are in agreement with the value deduced from dielectric measurements. The second process is observed in log E' as a shoulder after passing through the α process and prior to the melting. This behaviour also affects tan δ, broadening the peak and overlapping the α relaxation.

The different features observed in both runs concerning the last process are related to the different thermal histories applied to the sample. The sample was prepared by sintering the powdered polymer above 180°C and after cooling down to room temperature at a slow rate. The first heating run was performed up to the nematic phase. Immediately after, the sample was quickly cooled down to −150°C inside of the mechanical cell, before the second heating run. As a consequence of this thermal treatment, the sample contains a higher amorphous fraction, which exhibits a cold crystallization after crossing over the glass transition. This behaviour is not observed in the first heating scan. Besides, the cold crystallization causes a loss of elastic properties, giving rise to an increase in E'. A similar phenomenon is displayed by other LCP in shear loss factor as in shear modulus G' (ref. 29).

This behaviour is clearly observed in the d.s.c. curves at temperatures around 100°C. Above this temperature, and since this effect overlaps with the beginning of melting, the results of both contributions could generate the shoulder that appears in E'. These effects are clearly reflected in the dielectric measurements by means of the

thermal variation of $\epsilon'(T)$ above 80°C, even at low frequencies, as a consequence of the cold crystallization dynamics.

CONCLUSIONS

We have studied the thermal behaviour of a semicrystalline copper(II) metallomesogenic homopolymer, prior to studying the relaxation processes. Depending on the thermal history of the sample, two different glass transitions have been observed by d.s.c., which are associated with nematic and isotropic glasses, respectively. Besides, a cold crystallization appears before the melting and isotropization transitions. An α relaxation process is observed around the glass transition associated with the nematic glass. This process is better detected by d.m.t.a. measurements than by dielectric measurements since a conductivity contribution overlaps the α process. The polyester also exhibit a β relaxation below the glass transition corresponding with the motions of 4-hydroxybenzoate units and 4-hydroxybenzoic end-groups in this oligomeric polymer. The cold crystallization process and its kinetics are detected by mechanical and dielectric measurements.

ACKNOWLEDGEMENTS

This work is supported by the CICYT (Spain) under the projects MAT93-0104, MAT91-0923-C02-02 and MAT91-0695.

REFERENCES

1 Giroud-Godquin, A. M. and Maitlis, P. *Angew. Chem., Int. Edn. Engl.* 1991, **30**, 375
2 Espinet, P., Esteruelas, M. A., Oro, L. A., Serrano, J. L. and Sola, E. *Coord. Chem. Rev.* 1992, **117**, 215
3 Sirlin, C., Bosio, L. and Simon, J. *J. Chem. Soc. Commun.* 1987, 379
4 Stoessel, S. J. and Stille, J. K. *Macromolecules* 1992, **25**, 1832
5 Wright, M. E., Toplikar, E. G., Kubin, R. F. asnd Seltzer, M. D. *Macromolecules* 1992, **25**, 1838
6 Manriquez, J. M., Yee, G. J., McLean, R. S., Epstein, A. J. and Miller, J. S. *Science* 1991, **252**, 1415
7 Zuo, F., Yu, I., Salamon, M. B., Hong, X. and Stupp, S. I. *J. Appl. Phys.* 1991, **69**, 7951
8 Van der Pol, J. F., Neelam, E., Van Miltenburg, J. C., Zwikker, J. W., Nolte, R. J. M. and Drench, W. *Macromolecules* 1990, **23**, 155
9 Prasad, P. N. and Williams, D. J. 'Introduction to Nonlinear Optical Effects in Molecules and Polymers', Wiley, New York, 1991, p. 247
10 Dembek, A. A., Burch, R. R. and Feiring, A. E. *J. Am. Chem. Soc.* 1993, **115**, 2087
11 Takashashi, S., Murata, E., Kariya, M., Sonogashira, K. and Hagihara, N. *Macromolecules* 1979, **12**, 1016; Hanabusa, K., Kobayashi, C., Koyama, T., Masuda, E., Hirai, H., Kondo, Y., Takemoto, T., Fizuka, E. and Hojo, N. *Makromol. Chem.* 1986, **187**, 753
12 Carfagna, C., Caruso, U., Roviello, A. and Sirigu, A. *Makromol. Chem., Rapid Commun.* 1987, **8**, 345; Caruso, U., Roviello, A. and Sirugu, A. *Macromolecules* 1991, **24**, 2606
13 Hanabusa, K., Suzuki, T., Koyama, T., Shirai, H., Hojo, N. and Kurose, A. *Makromol. Chem.* 1990, **191**, 489; Zhou, Z., Dai, D. and Zhang, R. *Chin. J. Polym. Sci.* 1992, **10**, 70
14 Wiesemann, A., Zentel, R. and Pakula, T. *Polymer* 1992, **23**, 5315
15 Marcos, M., Oriol, L., Serrano, J. L., Alonso, P. J. and Puértolas, J. A. *Macromolecules* 1990, **23**, 5187
16 Marcos, M., Oriol, L. and Serrano, J. L. *Macromolecules* 1992, **25**, 5362
17 Alonso, P. J., Puértolas, J. A., Davidson, P., Martínez, B., Martínez, J. I., Oriol. L. and Serrano, J. L. *Macromolecules* 1993, **26**, 4304
18 Endres, B. W., Ebert, M., Wendorff, J. H., Reck, B. and
19 Ringsdorf, H. *Liq. Cryst.* 1990, 7, 217; Kremer, F., Vallerien, S. U., Zentel, R. and Kapitza, H. *Macromolecules* 1989, **22**, 4040
20 Green, D. I., Davies, G. R., Ward, I. M., Alhaj-Mohammed, M. H. and Abdul Jawad, S. *Polym. Adv. Technol.* 1990, **1**, 41; Kohler, W., Robello, D. R., Willard, C. S. and Williams, D. J. *Macromolecules* 1991, **24**, 4589
21 Chen, D. and Zachmann, H. G. *Polymer* 1991, **32**, 1612
22 Kovacs, A. J., Aklonis, J. J., Hutchinson, J. M. and Remos, A. R. *J. Polym. Sci., Polym. Phys. Edn* 1979, **17**, 2031
23 Hummel, J. P. and Flory, P. J. *Macromolecules* 1980, **13**, 479
24 Kalika, D. S. and Youn, D. Y. *Macromolecules* 1991, **24**, 3404
25 Kalika, D. S., Yoon, D. Y., Jannelli, P. and Parrich, W. *Macromolecules* 1991, **24**, 3413
26 Bottger, H. and Bryskin, U. V. 'Hopping Conduction in Solids', Akademie Verlag, Berlin, 1986
27 Kohler, W., Robello, D., Willand, C. and Williams, D. *Macromolecules* 1991, **24**, 4589
28 Tombari, E. and Cole, R. H. *J. Non-Cryst. Solids* 1991, **131–133**, 1125
29 MacCallum, J. R. and Vincent, C. A. 'Polymer Electrolytes Reviews', Elsevier, London, 1987, Vol. 1
30 Chem, D. and Zachmann, H. G. *Poymer* 1991, **32**, 1612